Available online at www.elixirpublishers.com (Elixir International Journal)

Mechanical Engineering

Elixir Mech. Engg. 49 (2012) 9734-9738

ISSN: 2229-712X

Modelling and evaluation of some effective parameters on reactor design for optimized utilization of ultrasonic waves

Ebrahim Fayyazi, Barat Ghobadian*,Gholamhassan Najafi, Bahram Hosseinzadeh and Mehdi Montazeri
Department of Mechanics of Agricultural Machinery, Tarbiat Modares University. Tehran, Iran.

ARTICLE INFO

Article history:
Received: 6 June 2012;
Received in revised form:
22 July 2012;
Accepted: 30 July 2012;

Keywords
Ultrasonic,
Reactor,
Cavitation,
Regression model,
Acoustic streaming.

ABSTRACT
Ultrasonic waves are used widely in food production, industry and chemical reactions. For conducting such a reactions, it is need to have a reactor in which liquid is affected by the waves. Among the most important parameters used for reactor design, the reactor dimensions may be considered as the most important parameter that can take influence the most, from the wave cavitation. In this study, effects of ultrasonic power, horn diameter and horn height on the amount of energy absorbed by liquid in reactor were evaluated and models were further developed for estimating the absorbed energy. Statistical analysis indicated that the effects of input power, reactor diameter and reactor height were all significant on energy absorption (P<0.01). The results revealed that as the horn diameter increased from 70 to 100 mm, 9% decrease was occurred in the absorbed energy. By increasing the horn height from 30 to 70 mm, 11% decrease was observed in the energy absorption. There was an 11% increase in the energy, together with an increase in ultrasonic wave power from 100 to 300 W. It was also concluded that the second order model was most suitable to predict the amount of energy absorbed by liquid (R^2=94.5%).

Introduction

When ultrasound travels through a medium, like any sound wave, it results in a series of compression and rarefaction. At sufficiently high power, the rarefaction may exceed the attractive forces between molecules in a liquid phase and, subsequently, result in the formation of cavitation bubbles. Each bubble affects the localized field experienced by neighboring bubbles.

Under such situations, the irregular field causes the cavitation bubble to become unstable and collapse, thereby releasing energy for chemical and mechanical effects. For example, in aqueous systems, at an ultrasonic frequency of 20 kHz, the collapse of each cavitation bubble acts as a localized "hotspot," generating enough energy to increase the temperature to about 4000 K and the pressure to values higher than 1000 atm. This bubble collapse, distributed through the medium, has a variety of effects within the system depending upon the type of material involved (Kuldiloke, 2002, Nyborg 1965, Pandit and Joshi, 1983).

The most significant sonochemical (including sonoelectrochemical) effects are connected with cavitation. Sonolysis needs cavitation collapse to generate high temperatures and pressures [Schram, 1991]. Ultrasonic activation of surfaces of reactants, catalysts and/or electrodes is connected with microjets formed by cavitation. Also acoustic streaming is connected with cavitation. It is evoked by radiation pressure, and is a consequence of absorption of the ultrasonic energy. This absorption is primarily a consequence of cavitation. There is no significant sonochemical effect without cavitation (Klıim et al.,2007, Kinsler and Frey 1962).

Ultrasonic waves are used widely in liquids. For example, in order to facilitate the chemical reactions and pasteurization in food materials the ultrasonic waves are applied. In ultrasonic application, it is necessary to design a reactor in which the desired liquid is affected by the waves. As a result of pressure variations and cavitation occurred in liquid, heat is produced that can be used as an index for designing a sonoreactor. To obtain such a condition, effect of various factors on the mentioned factor should be studied (Monnier et al., 1999).

In the case of acoustic cavitation, absorption of the ultrasonic wave during its propagation in the cavitating liquid is responsible for an energy gradient that induces a macroscopic liquid flow, called acoustic streaming (Bentitez, 2004).

Acoustic streaming causes the mixing effects experienced in the liquid, and therefore, it is important in the design of sonochemical reactors. An efficiency mixing is necessary, as there has been no transducer design that ensures a homogeneous distribution of the cavitation field within the reactor.

The value of mixing time can be determined by experimentation or by an empirical correlation, an example of the latter is the formula found by Vichare et al. (2001) and it's schematic diagram shown in Fig 1:

$$\theta_{mix} = 7\times10^{6} d^{-0.235}\left[\frac{Z^{\frac{3}{2}}T^{3}(T+2Z)^{-2}d_h^{-4}}{v_h^{2}g^{\frac{1}{2}}\mu^{-2}\rho_l^{2}}\right] \quad (1)$$

θ_{mix} = mixing time, s
d = Jet length, m
Z = height of liquid in the beaker, m
T = diameter of beaker, m
d_h = diameter of the horn, m
v_h = velocity of the horn, m/s
g = acceleration due to gravity, m/s^2
μ= viscosity of liquid, Ns/m^2
ρ_l = Density of liquid, kg/m^3

Tele: +982148290
E-mail addresses: Ghobadianb@modares.ac.ir

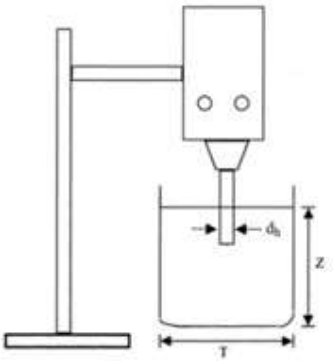

Fig. 1. Schematic representation of apparatus and reactor used for conducting experiments

The intensity of sonication is directly proportional to the square of the amplitude of vibration of the ultrasonic source (Mason, 1999, Carlin et al., 1972, Shutilov, 1988).

In the case of planar waves, I (W/m^2), is given by:

$$I = \frac{\rho_l c\left(a^2(2\pi f)^2\right)}{2} \qquad (2)$$

c = Velocity of the sound in the liquid, m/s

a = Amplitude of oscillation of the horn, m

f = Frequency of ultrasound, Hz

For this system the temperature is recorded against time, at intervals of a few seconds, using a thermocouple placed in the reaction itself. From the temperature, K, versus time, t, the temperature rise at time zero,(dK/dt), is determined as (Benitez, 2004):

$$Power = \left(\frac{dK}{dt}\right)_0 C_p m \qquad (3)$$

C_p = Heat capacity of the solvent, J. kg^{-1}. K^{-1}

m = mass of solvent used, kg

If this power is dissipated into the system from a probe tip with an area measured in cm^2, A, then the Intensity of Power, I (W/cm^2), is given by Benitez (2004):

$$I = \frac{Power}{A} \qquad (4)$$

Intensity of ultrasound can be determined by Eq. (4). Substitution of this value in Eq. (2) gives the amplitude of horn oscillations (a). The mean velocity of the net fluid displacement from the vibrating horn face, v_h in m/s, from the planar wave analysis can be computed as Vichare et al. (2001):

$$v_h = af \qquad (5)$$

According to Eqs. (1-5), the important parameters for designing a reactor are Z, T, Power and d_h. In this study, d_h is constant; while effects of T, Z, and Power are evaluated as effective independent variables on the amount of energy absorbed by the water in the reactor.

Material and Methods

An ultrasonic generator (Hielscher, Model UP400S) with a frequency of 24 kHz and 400 W power was used for this research work. A titanium sonotrode with diameter of 16 mm was used. Before starting the experiments, the temperature was set at 24 °C. Three sampling cylinders with 60 mm diameter and 40 mm height were selected and covered to be insulated from head exchange with environment. These cylinders form the reactor. The experimental water container was put at room temperature to be equilibrated with room temperature. Water samples with defined height were poured in the reactor and treated by ultrasonic waves. The temperature variations were recorded every 10 seconds by a thermometer and the amount of absorbed energy by the water was determined considering the temperature variations in the reactor water. Independent variables studied in the research were shown on Table (1). Finally, the recorded data was analyzed using statistical software.

Table 1. Independent variables studied in the research.

Levels			Source
300	200	100	Input Power (W)
70	50	30	Height (mm)
100	85	70	Diameter (mm)

Results and discussion

Results of statistical analysis indicated that the effects of input power, reactor diameter and reactor height and also the interaction effect of reactor height and input power were significant on 1% level (Table 2). This shows that the evaluated factors in this study were accurately selected for designing the reactor.

Table 2.Variance analysis of specific Absorption Energy

Source	DF	Sum of squares	MSE	F
Diameter (mm)	2	142497930	71248965	196.51^{**}
Height (mm)	2	174387284	87193642	240.48^{**}
Power (W)	2	160993272	80496636	222.01^{**}
Diameter*Height	4	3317967	829492	2.29^{ns}
Diameter*Power	4	428100	107025	0.30^{ns}
Height*Power	4	6124458	1531114	4.22^{**}
Error	62	22479797	362577	
Total	80	510228807		
* and ** significant in 1% and 5% level, respectively; ns: not significant				

By increasing the diameter of the reactor from 70 to 85 and 100 mm, the amount of absorbed specific energy decreased 7% and 9%, respectively (Fig.2). The amount of specific energy decreased 5% and 11% by increasing the reactor height from 30 to 50 and 70 mm, respectively (Fig. 3).

Other researchers reported almost the similar results about the effect of reactor dimensions on string time and cavitation (Vichare et al., 2001 and Klıim et al., 2007).

Increasing the reactor diameter and height caused a decrease in the ratio of effective volume by the sonotrode to the total volume of the water in the reactor. The created flow in the reactor stirs the water and consequently, cause temperature transmission to untreated water in the reactor. According to Eq. (1), by increasing the reactor diameter and height, stirring time increases and the effect of sonotorde on the water components decrease. The variation of specific energy absorbed by the water versus variation of the reactor diameter and height is illustrated in Fig. 4.

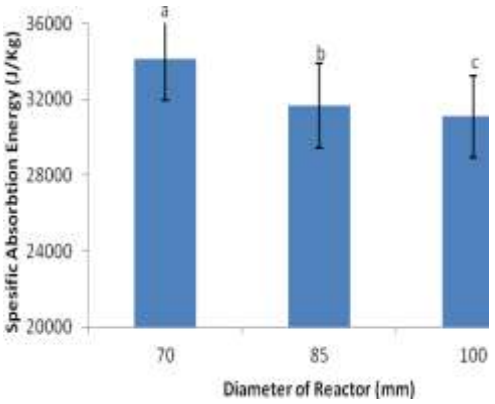

Fig. 2. Effect of the Reactor Diameter on Specific Absorption Energy (Different letters in each column shows significant difference at 1% probability level (LSD))

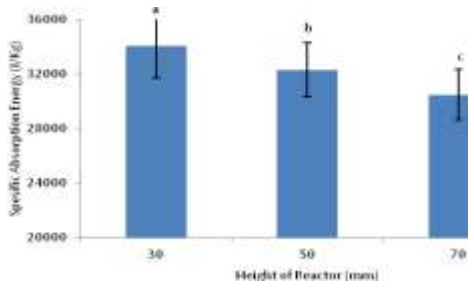

Fig. 3. Effect of the Reactor height on Specific Absorption Energy (Different letters in each column shows significant difference at 1% probability level (LSD))

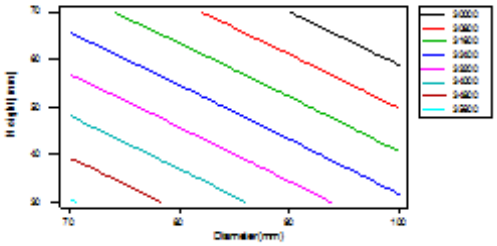

Fig. 4. Contour plot showing the effect of Diameter and height on specific absorption energy

By increasing the input power from 100 W to 200 and 300 W, the amount of specific absorbed energy increased 6% and 11%, respectively (Fig. 5). Based on the results obtained by LSD Test, the effect of input power was significant on the specific absorbed energy. As the volume of the water in the reactor increased from 120 to 550 cc, due to a decrease in ultrasonic wave's effect, 23% decrease was observed in the amount of absorbed energy. This decrease is observable at all of the volume and power levels evaluated. Eq. (6) was obtained to estimate the amount of energy absorption considering variations in volume and power and also the data presented in Table 3.

Table 3. Estimated Regression (Linear Logarithmic) Coefficients for Specific Absorption Energy

Term	Coefficient	SE Coefficient	P
Constant	-19322	2615	0.000**
Ln (Volume)	-4313.2	269.1	0.000**
Ln (Power)	3090.1	265.3	0.000**

Standard Error = 625.3 R^2 = 94.2%

SAE = - 19322 – 4313×Ln V + 3090×Ln P (6)

SAE= Specific Absorption Energy (J/kh)

V= Volume (m^3)

P= Input Power (W)

Fig. 6 shows the interaction effect of power and reactor height on specific absorbed energy. At the height of 30 mm, the specific absorbed energy increases with more inclination versus the power. This is due to the fact that during the water stirring process in the reactor, the height is traversed twice compared with the reactor diameter. Considering Eq. (7), the reactor height is more effective on specific absorbed energy in comparison with its diameter.

$$L = T + 2Z \quad (7)$$

L=loop length

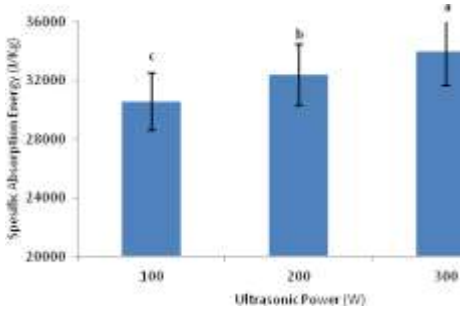

Fig. 5. Effect of the ultrasonic power on Specific Absorption Energy (Different letters in each column shows significant difference at 1% probability level (LSD))

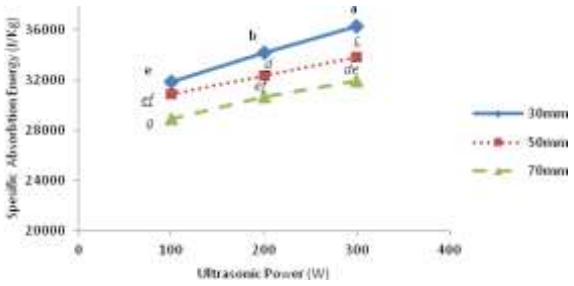

Fig. 6. Interaction effect of ultrasonic power and reactor height on specific absorption energy (Different letters in each column shows significant difference at 1% probability level (LSD))

The variation of specific absorbed energy versus the reactor diameter, power and height are illustrated in Figs. (7and 8).

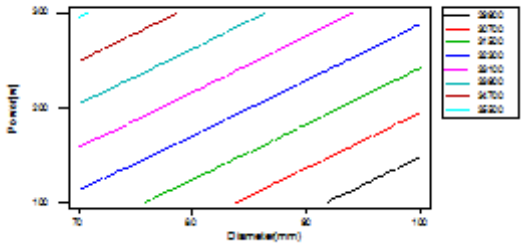

Fig. 7. Contour plot showing the effect of Diameter and power on specific absorption energy.

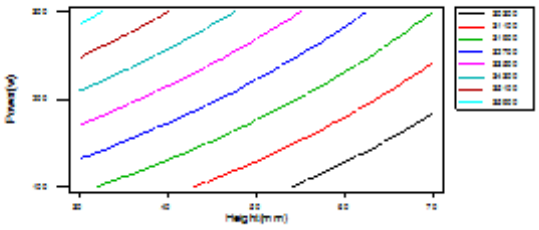

Fig. 8. Contour plot showing the effect of power and height on specific absorption energy.

Fig. 9 shows the amount of absorbed energy during the treatment time. Within the first 60 s, the differential amount of specific absorbed energy has ascending inclination. By increasing the water temperature in the reactor, the amount of specific absorbed energy decreases. During the experiment process, from 20 to 60 s, 41% increase is occurred in the specific absorbed energy, while after the time of 60 s, the specific

absorbed energy decreases 19%. Because the amount of energy decrease is remarkably less than initial increase in the energy, the aggregate amount of absorbed energy increases with an approximately constant trend.

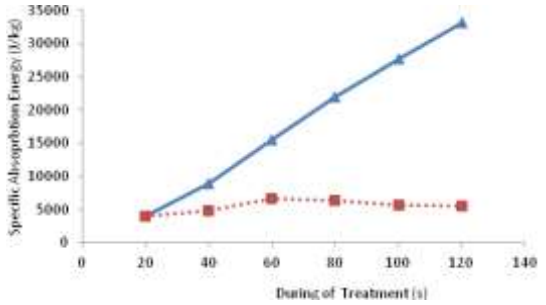

Fig. 9. Cumulative of specific absorption energy on during of treatment (▲) and amount of specific absorption energy on each 20 seconds (■.).

According to Table 4 and regarding to significance of regression model and also high difference between the model sum of squares (SS) and residual error (RE), it could be concluded that this model can be used to predict the amount of specific absorbed energy with variables of diameter, height and input power. In Tables 5 to 8 different regression models are presented.

Table 4. Analysis of Variance for Specific Absorption Energy

Source	DF	Sum of squares	MSE	F
Regression	9	482239945	53582216	135.92**
Linear	3	460921234	9416627	23.89**
Square	3	16957252	5652417	14.34**
Interaction	3	4361459	1453820	3.69*
Residual Error	71	27988862	394209	
Total	80	510228807		

Table 5. Estimated Regression (Linear) Coefficients for Specific Absorption Energy

Term	Coefficient	SE Coefficient	P
Constant	42001.4	714.314	0.000**
Diameter (mm)	-101.8	7.260	0.000**
Height (mm)	-89.8	5.445	0.000**
Power(w)	17.3	1.089	0.000**

Standard Error = 800.2 R^2 = 90.3%

SAE=42001.4-101.8×T-80.9×Z+17.3×P (8)

Table 6. Estimated Regression (Linear+Square) Coefficients for Specific Absorption Energy .

Term	Coefficient	SE Coefficient	P
Constant	71617.9	5038.77	0.000**
Diameter (mm)	-828.3	117.90	0.000**
Height (mm)	-80.9	39.22	0.043ns
Power(w)	22.3	6.30	0.001**
Diameter*Diameter	4.3	0.69	0.000**
Height*Height	-0.1	0.39	0.820ns
Power(w)*Power	-0.0	0.02	0.419**

Standard Error =661.2 R^2 =93.7%

SAE=71617.9-828.3×T-80.9×Z+22.3×P+4.3×T^2 (9)

Table 7. Estimated Regression (Linear+Interaction) Coefficients for Specific Absorption Energy.

Term	Coefficient	SE Coefficient	P
Constant	40383.2	2541.43	0.000**
Diameter (mm)	-103.1	28.61	0.001**
Height (mm)	-63.3	39.39	0.113ns
Power(w)	27.3	8.11	0.001**
Diameter*Height	0.1	0.43	0.828ns
Diameter*Power	-0.0	0.09	0.845ns
Height*Power	-0.2	0.05	0.009**

Standard Error = 779.3 R^2 =91.2%

SAE=40383.2-103.1×T+27.3×P-0.2×Z×P (10)

Table 8. Estimated Regression (Full Quadratic) Coefficients for Specific Absorption Energy

Term	Coefficient	SE Coefficient	P
Constant	69999.7	5174.19	0.000**
Diameter (mm)	-829.7	114.16	0.000**
Height (mm)	-54.4	48.74	0.268ns
Power(w)	32.4	8.82	0.000**
Diameter*Diameter	4.3	0.66	0.000**
Height*Height	-0.1	0.37	0.811ns
Power(w)*Power	-0.0	0.01	0.394ns
Diameter*Height	0.1	0.35	0.788ns
Diameter*Power	-0.0	0.07	0.808ns
Height*Power	-0.2	0.05	0.001**

Standard Error = 627.9 R^2 =94.5

SAE=69999.7-829.7×T+32.4×P+4.3×T^2-0.2×Z×P (11)

Considering the values of R^2 and standard error (SE) of Eqs (8-11) are shown that the "full quadratic" model is the best regression model to estimate the amount of specific absorbed energy.

The significance of regression model and also high difference between sum of squares (SS) and residual error (RE) of the model proves that the model is useful for estimating the temperature using variables of input power, time and liquid volume. Different regression models in this case are given in Tables 9 to 13.

Table 9. Analysis of Variance for temperature

Source	DF	Sum of squares	MSE	F
Regression	9	984.459	109.3843	5000**
Linear	3	983.376	10.1492	492.89**
Square	3	0.649	0.2163	10.50**
Interaction	3	0.434	0.1448	7.03**
Residual Error	152	3.130	0.0206	
Total	161	987.589		

Table 10. Estimated Regression (Linear) Coefficients for temperature

Term	Coefficient	SE Coefficient	P
Constant	15	0.052	0.000**
Power(w)	0.07	0.000	0.000**
Time (s)	0.004	0.000	0.000**
Volume (m^3)	-2234	100.340	0.000**

Standard Error = 0.1633 R^2 =99.6%

SAE=15+0.07×P+0.004×t-2234×V (12)

Table 11. Estimated Regression (Linear+Square) Coefficients for temperature

Term	Coefficient	SE Coefficient	P
Constant	16	0	0.000**
Power(w)	0.04	0	0.000**
Time (s)	0.003	0	0.043*
Volume (m^3)	-4649	465	0.001**
Power*Power	0.005	0	0.000**
Time*Time	-0.01	0	0.820ns
Volume*Volume	3660058	691040	0.419ns

Standard Error = 661.2 R^2 =93.7%

SAE=16+0.04P+0.003t-4649V+0.005P^2 (13)

Table 12. Estimated Regression (Linear+Interaction) Coefficients for temperature

Term	Coefficient	SE Coefficient	P
Constant	15	0.119	0.000**
Power(w)	0.08	0.000	0.000**
Time (s)	0.012	0.001	0.000**
Volume (m^3)	-1604	321.087	0.000**
Power* Time	0.002	0.000	0.002**
Power*Volume	-0.001	1.175	0.705ns
Time *Volume	-8	2.809	0.007**

Standard Error = 0.1561 R^2 =99.6%

$$SAE=15+0.08+0.012\times t-1604\times V+0.002\times P\times t-8\times t\times V \quad (14)$$

Table 13. Estimated Regression (Full Quadratic) Coefficients for temperature

Term	Coefficient	SE Coefficient	P
Constant	16	0	0.000^{**}
Power(w)	0.09	0	0.004^{**}
Time (s)	0.003	0	0.000^{**}
Volume (m^3)	-4018	523	0.000^{**}
Power*Power	0.001	0	0.867^{ns}
Time*Time	-0.02	0	0.697^{ns}
Volume*Volume	3660058	653932	0.000^{**}
Power* Time	0.002	0	0.001^{**}
Power*Volume	-0.001	1	0.681^{ns}
Time *Volume	-8	3	0.003^{**}

Standard Error = 0.1435 R^2 =99.7%

$$SAE=16+0.09\times P+0.003\times t-4018\times V+3660058\times V^2+0.002\times P\times t-8\times t\times V \quad (15)$$

Considering the values of R^2 and standard error (SE) of Eqs (12-15) are shown that The "Full Quadratic" and "Linear+Interaction" models (with R^2 values of 99.7% and 99.6% and standard errors of 0.1435 and 0.1561, respectively) were better models in comparison with "Linear" and "Linear+Square" models to predict the water temperature in the reactor at different experimental times.

Conclusion

1- Results of statistical analysis indicated that the effects of input power, reactor diameter and reactor height were significant on 1% level. This shows that the evaluated factors in this study were accurately selected for designing the reactor.

2- By increasing the diameter of the reactor from 70 to 85 and 100 mm, the amount of absorbed specific energy decreased 7% and 9%, respectively.The amount of specific energy decreased 5% and 11% by increasing the reactor height from 30 to 50 and 70 mm, respectively. Increasing the reactor diameter and height caused a decrease in the ratio of effective volume by the sonotrode to the total volume of the water in the reactor.

3- By increasing the input power from 100 W to 200 and 300 W, the amount of specific absorbed energy increased 6% and 11%, respectively

4- At the height of 30 mm, the specific absorbed energy increases with more inclination versus the power. This is due to the fact that during the water stirring process in the reactor, the height is traversed twice as compared with the reactor diameter.

References

1-Bentitez FA (2004). Effects of the use of ultrasonic waves on biodiesel production in alkaline transesterification of bleached tallow and vegetable oils: cavitation model, doctor of philosophy thesis.University of Puerto Rico.

2-Carlin B (1972). Ultrasonica. Ediciones URMO. Spain.

3-Benitez FA,(2004). Effects of the use ultrasonic waves on biodiesel production in alkaline transesterification if bleched tallow and vegetable oils: cavitation model, Ph.D thesis, University of Puerto Rico.

4-Kinsler LE, Frey AR (1962). Fundamental of Acoustics, second edn. Wiley. New York.

5-Klıim J, Frias-Ferrer A, Gonzalez-Garcia J, Saez LV, Iniesta J (2007). Optimisation of 20 kHz sonoreactor geometry on the basis of numerical simulation of local ultrasonic intensity and qualitative comparison with experimental results. Ultrasonics Sonochemistry. 14:19-28.

6-Kuldiloke J (2002). Effect of ultrasound, temperature and pressure treatments on enzyme activity and quality indicators of fruit and vegetable juices, M.Sc.Thesis, Institute of Food Technology Food biotechnology and process technology the Technical University of Berlin.

7-Mason TJ (1999). Sonochemistry. Oxford University Press. New York.

8-Monnier H, Wilehlm AM, Delmas H (1999). The infuence of ultrasound on micromixing in a stirred batch reactor, Chem. Engng. Sci. 13-14.

9-Nyborg WL (V). Acoustic streaming, Physical Acoustics Principles and Methods. Academic Press. New York. London.

10- Pandit AB, Joshi JB (1983). Mixing in mechanically agitated gas-liquid contactors, bubble columns and modi®ed bubble columns, Chem. Engng. Sci. 38 (8): 1189-1215.

11- Schram CJ (1991) Manipulation of particles in an acoustic field. Advances in Sonochemistry, vol. 2, JAI Press, London. 293-322.

12- Shutilov VA (1988). Fundamentals physics of ultrasound, Gordon and Breach science publishers. Amsterdam.

13- Vichare NP, Gogate PR, Dindore VD, Pandit A B (2001). Mixing time analysis of a sonochemical reactor. Ultrasonics Sonochemistry.8:23-33.